Impact Factors for Fatigue Design of Steel I-Girder Bridges Considering the Deterioration of Road Surface Condition

Wei Wang[1] and Lu Deng, Ph.D., M.ASCE[2]

Abstract: The purpose of this paper is to evaluate the impact factor (IM) in LRFD bridge design specifications for fatigue design and to propose a method for determining reasonable IMs for the fatigue design of steel I-girder bridges that can more rationally consider the effect of the deterioration of the road surface condition (RSC) during its whole lifecycle. The deterioration process of the RSC was investigated under the given traffic and environmental conditions, and the number of truck passages taken for the RSC to deteriorate from one class to the next was investigated. A three-dimensional coupled vehicle–bridge model was developed to simulate the interaction between the bridge and vehicle, with both the bridge and fatigue load models adopted from an existing LRFD code. The IM of the stress range ($IM_{\_SR}$), which is calculated using the stress range instead of the maximum stress used traditionally, was used for the fatigue analysis of steel girders. Numerical simulations were performed to study the $IM_{\_SR}$ of steel I-girder bridges under different RSCs while taking into consideration the effect of two other important parameters: bridge span length and vehicle speed. Results show that the RSC has a greater impact on the $IM_{\_SR}$ than on the traditional IM, and the $IM_{\_SR}$ is greater than the traditional IM calculated using the maximum stress. By considering the cumulative fatigue damage caused by the passage of each truck under different RSCs and the deterioration process of the RSC during its whole lifecycle, simple and reasonable expressions were proposed for the IMs for fatigue design of steel I-girder bridges under the given traffic and environmental conditions.
DOI: 10.1061/(ASCE)BE.1943-5592.0000885.

Author keywords: Impact factor; Fatigue design; Deterioration process; Road surface condition; Steel I-girder bridge.

Introduction

The fatigue life of steel bridge girders is dominated by the stresses caused by the trucks crossing the bridge. The stress range (an algebraic difference between the maximum and minimum stresses) due to each truck passage and the number of stress cycles are two key parameters in the fatigue analysis. In the current AASHTO LRFD bridge design specifications (AASHTO 2012), the stress range for fatigue design is calculated by applying an impact factor (IM) of 0.15 to the calculated static stress range caused by the passage of the specified fatigue truck. This IM of 0.15 adopted in the current AASHTO LRFD code for fatigue design was based on the numerical simulation results of Hwang and Nowak (1991), in which four steel I-girder composite bridges with span lengths between 12 and 30 m were studied while an average road surface condition (RSC) was adopted. However, previous studies have shown that the real stress ranges of bridge components due to the dynamic vehicle loading can be significantly underestimated when the RSC is poor (Rao and Talukdar 2003; Zhang and Cai 2012; Zhang and Cai 2013). Therefore, the IM of 0.15 currently adopted in the AASHTO LRFD code (AASHTO 2012) may not truly reflect the dynamic effect of vehicle loading on the stress ranges of bridge components during the whole lifecycle of a RSC.

During the service life of a steel bridge, the dynamic impacts due to the traffic loads and deteriorated RSCs can induce serious fatigue issues for the bridge components (Zhang and Cai 2012). Although there have been a number of studies on the effect of RSC on the behavior of vehicle–bridge systems (Deng and Cai 2010a; O'Brien et al. 2006; Schenk et al. 2003; da Silva 2004) and other related applications, such as vehicle load or parameter identification (Deng and Cai 2009; Deng and Cai 2010b; Wu and Law 2011) and bridge damage detection (Jaksic et al. 2014), few studies have investigated the effect of the road-surface deterioration process on the fatigue behavior of steel bridges. Zhang and Cai (2012, 2013) studied the effect of vehicle speed and RSC on the fatigue life of a steel bridge and proposed an approach for the fatigue design of steel bridges in which the equivalent stress ranges induced by each truck passage and the number of stress cycles were combined into one variable based on the equivalent fatigue damage. They found that the road-surface deterioration rate had a significant influence on the fatigue reliability of bridge components. However, the deterioration process of the RSC was only considered qualitatively in their study, and the cause for the deterioration of RSC, i.e., the cumulative fatigue damage by each truck passage during its whole lifecycle, was not considered in their study, which may lead to inaccurate predicted fatigue life.

The purpose of this paper is to evaluate the IM specified in the AASHTO LRFD code for bridge-fatigue design and propose a method for determining reasonable IMs for the fatigue design ($IMs_{\_FD}$) of steel I-girder bridges that can more rationally consider the effect of the deterioration of the RSC during the whole lifecycle. The paper is organized in three main parts. First, under the given traffic and environmental conditions, the deterioration process of the RSC is investigated in terms of the number of truck passages and the time taken for the RSC to deteriorate from one class to the next, for instance, from the good class to the average class. Second, a three-dimensional coupled vehicle–bridge model is developed to

[1]Graduate Student, College of Civil Engineering, Hunan Univ., Changsha, Hunan 410082, China. E-mail: jswnww@hnu.edu.cn

[2]Professor, Key Laboratory for Wind and Bridge Engineering of Hunan Province, Hunan Univ., Changsha, Hunan 410082, China (corresponding author). E-mail: denglu@hnu.edu.cn

Note. This manuscript was submitted on May 25, 2015; approved on October 28, 2015; published online on January 22, 2016. Discussion period open until June 22, 2016; separate discussions must be submitted for individual papers. This paper is part of the ***Journal of Bridge Engineering***, © ASCE, ISSN 1084-0702.

analyze the IM of the stress range ($IM_{\_SR}$) of the steel I-girder bridges under consideration. The relationships among three parameters, including the bridge span length, RSC, and vehicle speed, and the $IM_{\_SR}$ were investigated by numerical simulations. Finally, simple and reasonable expressions of the $IMs_{\_FD}$ for steel I-girder bridges are proposed.

Analytical Bridges

In this study, five typical steel I-girder bridges with span lengths ranging from 10.67 m (35 ft) to 36.58 m (120 ft) were designed according to the AASHTO LRFD bridge design specifications (AASHTO 2012). All five bridges, each consisting of five identical girders with a girder spacing of 2.13 m (7 ft), are simply supported and have a roadway width of 9.75 m (32 ft) and a bridge-deck thickness of 0.20 m (8 in). A typical cross section of the bridges is shown in Fig. 1. Besides the end diaphragms, which are used for all five bridges, intermediate diaphragms are also used to connect the five girders depending on their span lengths, as provided in Table 1. In this study, the steel I-girder bridges were modeled with *ANSYS 14.5*. Fig. 2 shows the finite-element model of Bridge 2. A summary of the detailed properties and the fundamental frequencies of the five bridges obtained from the modal analysis is provided in Table 1.

Analytical Vehicle Model

The HS20-44 truck specified in the AASHTO LRFD bridge design specifications (AASHTO 2012) was used as the fatigue truck for the five bridges. The analytical model for this truck is illustrated in Fig. 3. The properties of the truck, including the geometry, mass distribution, damping, and stiffness of the tires and suspension systems, are given in Table 2 (Shi 2006).

Coupled Vehicle–Bridge System

Equation of Motion of the Vehicle

The equation of motion for a vehicle can be expressed as follows:

$$[M_v]\{\ddot{d}_v\} + [C_v]\{\dot{d}_v\} + [K_v]\{d_v\} = \{F_G\} + \{F_v\} \quad (1)$$

where $[M_v]$, $[C_v]$, and $[K_v]$ = mass, damping, and stiffness matrices of the vehicle, respectively; $\{d_v\}$ = displacement vector of the vehicle; $\{F_G\}$ = gravity force vector of the vehicle; and $\{F_v\}$ = vector of the wheel–road contact forces acting on the vehicle.

Equation of Motion of the Bridge

The equation of motion for a bridge can be written as follows:

$$[M_b]\{\ddot{d}_b\} + [C_b]\{\dot{d}_b\} + [K_b]\{d_b\} = \{F_b\} \quad (2)$$

where $[M_b]$, $[C_b]$, and $[K_b]$ = mass, damping, and stiffness matrices of the bridge, respectively; $\{d_b\}$ = displacement vector of the bridge; and $\{F_b\}$ = vector of the wheel–road contact forces acting on the bridge.

Assembling the Vehicle–Bridge Coupled System

Based on the displacement relationship and the interaction force relationship at the contact points, the vehicle–bridge Coupled system can be established by combining the equations of motion of both the bridge and vehicle (Deng and Cai 2009)

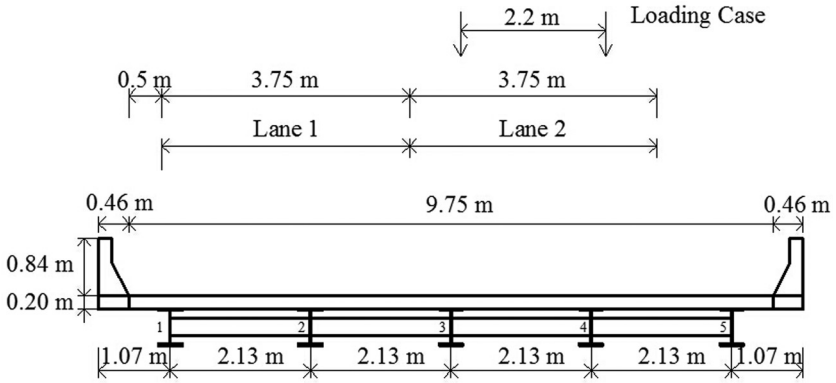

Fig. 1. Typical cross section of bridges considered and vehicle loading position adopted

Table 1. Detailed Properties of the Five Bridges

Bridge	Span length (m)	Fundamental natural frequency (Hz)	Girder		No. of intermediate diaphragms
			Cross-sectional area (m^2)	Inertia moment of cross section (10^{-2} m^4)	
1	10.67	12.40	0.018	0.040	1
2	16.76	8.62	0.020	0.109	2
3	22.86	6.10	0.023	0.219	2
4	30.48	4.39	0.026	0.421	3
5	36.58	3.49	0.028	0.641	4

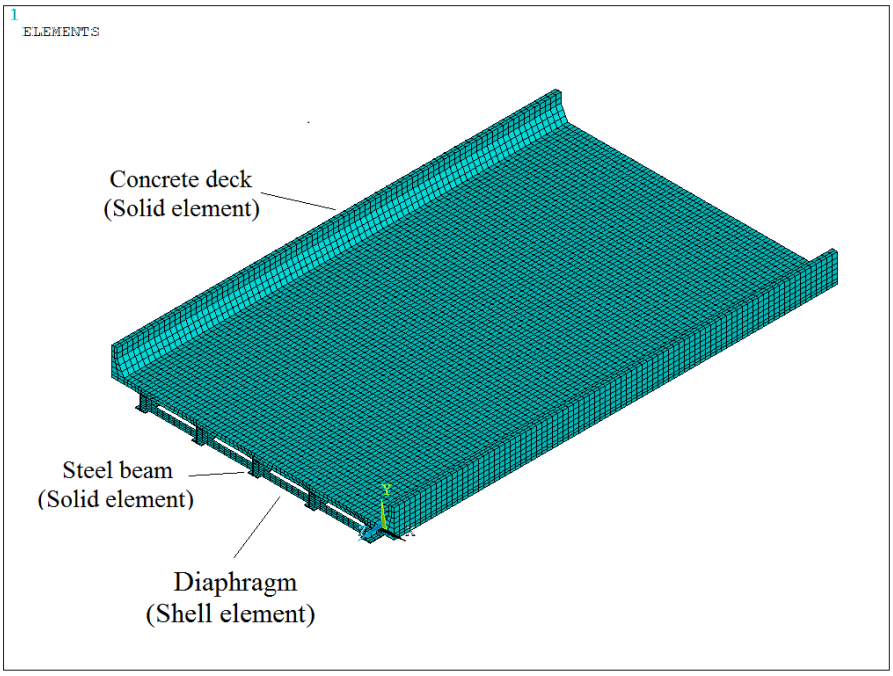

Fig. 2. Finite-element model for Bridge 2

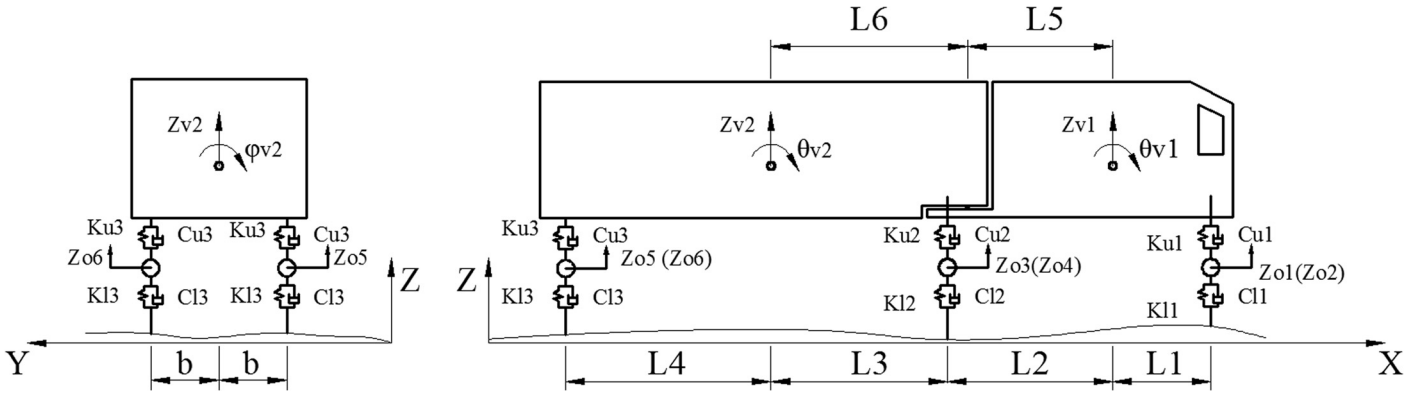

Fig. 3. Analytical model of the fatigue truck

$$\begin{bmatrix} M_b & \\ & M_v \end{bmatrix} \begin{Bmatrix} \ddot{d}_b \\ \ddot{d}_v \end{Bmatrix} + \begin{bmatrix} C_b + C_{b-b} & C_{b-v} \\ C_{v-b} & C_v \end{bmatrix} \begin{Bmatrix} \dot{d}_b \\ \dot{d}_v \end{Bmatrix} + \begin{bmatrix} K_b + K_{b-b} & K_{b-v} \\ K_{v-b} & K_v \end{bmatrix} \begin{Bmatrix} d_b \\ d_v \end{Bmatrix} = \begin{Bmatrix} F_{b-r} \\ F_{v-r} + F_G \end{Bmatrix} \tag{3}$$

where C_{b-b}, C_{b-v}, C_{v-b}, K_{b-b}, K_{b-v}, K_{v-b}, F_{b-r}, and F_{v-r} are due to the wheel–road contact forces and are time-dependent terms.

To simplify the bridge model and therefore save computational effort, the modal superposition technique can be used (Deng and Cai 2010b), and Eq. (3) can be simplified into the following:

$$\begin{bmatrix} I & \\ & M_v \end{bmatrix} \begin{Bmatrix} \ddot{\xi}_b \\ \ddot{d}_v \end{Bmatrix} + \begin{bmatrix} 2\omega_i \eta_i I + \Phi_b^T C_{b-b} \Phi_b & \Phi_b^T C_{b-v} \\ C_{v-b} \Phi_b & C_v \end{bmatrix} \begin{Bmatrix} \dot{\xi}_b \\ \dot{d}_v \end{Bmatrix} + \begin{bmatrix} \omega_i^2 I + \Phi_b^T K_{b-b} \Phi_b & \Phi_b^T K_{b-v} \\ K_{v-b} \Phi_b & K_v \end{bmatrix} \begin{Bmatrix} \xi_b \\ d_v \end{Bmatrix} = \begin{Bmatrix} \Phi_b^T F_{b-r} \\ F_{v-r} + F_G \end{Bmatrix} \tag{4}$$

After obtaining the bridge dynamic responses, the stress vector can be obtained by

$$[S] = [E][B]\{d_b\} \tag{5}$$

where $[E]$ is the stress–strain relationship matrix and is assumed to be constant over the element; and $[B]$ is the strain-displacement relationship matrix assembled with x, y, and z derivatives of the element shape functions.

Modeling the Deterioration Process of RSC

Generation of Road Surface Profile

RSC is a very important factor that affects the dynamic interaction between the bridge and vehicle. A road surface profile is usually assumed to be a zero-mean stationary Gaussian random process and can be generated through an inverse Fourier transformation based

Table 2. Major Parameters of the Fatigue Truck Model Used in This Study

Parameter	Value
Mass of Truck Body 1 (kg)	2,612
Pitching moment of inertia of Truck Body 1 (kg·m^2)	2,022
Rolling moment of inertia of Tuck Body 1 (kg·m^2)	8,544
Mass of Truck Body 2 (kg)	26,113
Pitching moment of inertia of Truck Body 2 (kg·m^2)	33,153
Rolling moment of inertia of Tuck Body 2 (kg·m^2)	181,216
Mass of first axle suspension (kg)	490
Upper spring stiffness of first axle (N/m)	242,604
Upper damper coefficient of first axle (N·s/m)	2,190
Lower spring stiffness of first axle (N/m)	875,082
Lower damper coefficient of first axle (N·s/m)	2,000
Mass of second axle suspension (kg)	808
Upper spring stiffness of second axle (N/m)	1,903,172
Upper damper coefficient of second axle (N·s/m)	7,882
Lower spring stiffness of second axle (N/m)	3,503,307
Lower damper coefficient of second axle (N·s/m)	2,000
Mass of third axle suspension (kg)	653
Upper spring stiffness of third axle (N/m)	1,969,034
Upper damper coefficient of third axle (N·s/m)	7,182
Lower spring stiffness of third axle (N/m)	3,507,429
Lower damper coefficient of third axle (N·s/m)	2,000
Distance from front axle to mass center of tractor L1 (m)	1.698
Distance from middle axle to mass center of tractor L2 (m)	2.569
Distance from middle axle to mass center of trailer L3 (m)	4.452
Distance from rear axle to mass center of trailer L4 (m)	4.692
Distance from rivet joint to mass center of tractor L5 (m)	2.215
Distance from rivet joint to mass center of trailer L6 (m)	4.806
Half distance between wheels in the same axle b (m)	1.1

Table 3. RRCs for Different Road-Roughness Classifications

Road-roughness classification	Range for RRC (m^3/cycle)
Very good	2×10^{-6} to 8×10^{-6}
Good	8×10^{-6} to 32×10^{-6}
Average	32×10^{-6} to 128×10^{-6}
Poor	128×10^{-6} to 512×10^{-6}
Very poor	512×10^{-6} to $2{,}048 \times 10^{-6}$

Table 4. Number of Truck Passages and Time Taken for the RSC to Deteriorate to the Next Class

	RSC				
Parameter	Very good	Good	Average	Poor	Very poor
N_i	4,113,464	1,156,504	938,321	839,119	768,396
t_i (years)	6.63	1.86	1.52	1.35	1.24
T (years)	6.63	8.49	10.01	11.36	12.6
r_i (%)	52.63	14.80	12.01	10.74	9.82

on a power spectral density (PSD) function (Dodds and Robson 1973) such as

$$r(X) = \sum_{k=1}^{N} \sqrt{2\varphi(n_k)\Delta n}\cos(2\pi n_k X + \theta_k) \tag{6}$$

where θ_k is the random phase angle uniformly distributed from 0 to 2π; $\varphi()$ is the PSD function (m^3/cycle/m) for the road surface elevation; and n_k is the wave number (cycles/m). In this study, the following PSD function was used (Huang and Wang 1992):

$$\varphi(n) = \varphi(n_0)\left(\frac{n}{n_0}\right)^{-2} \quad (n_1 < n < n_2) \tag{7}$$

where n is the spatial frequency (cycles/m); n_0 is the discontinuity frequency of $1/2\pi$(cycles/m); $\varphi(n_0)$ is the roughness coefficient (m^3/cycle) whose value is chosen depending on the road condition; and n_1 and n_2 are the lower and upper cutoff frequencies, respectively.

Index of RSC

RSC can be described with the present serviceability rating (PSR), road-roughness coefficient (RRC), or international roughness index (IRI) (Paterson 1986; Shiyab 2007). Both the PSR and RRC classify the RSC into five categories: very good, good, fair (average), poor, and very poor. However, the PSR is based on the passenger's interpretation of ride quality, which is developed by the AASHTO road test, whereas the RRC is based on the road profile only. ISO (1995) used the RRC to define the road-roughness classification with the ranges for different classes listed in Table 3. Similar to the RRC, the IRI developed in 1986 is used to define the longitudinal profile of a wheel track (Paterson 1986; Sayers and Karamihas 2007), and it is based on the average rectified slope, which is a filtered ratio of a standard vehicle's accumulated suspension motion divided by the distance traveled by the vehicle during the measurement. Various correlations have been developed between those indices (Paterson 1986; Shiyab 2007). In this study, the relationship between the IRI and RRC developed by Shiyab (2007) was adopted

$$\varphi(n_0) = 6.1972 \times 10^{-9} \times e^{\mathrm{IRI}/0.42808} + 2 \times 10^{-6} \tag{8}$$

Progressive Deterioration of RSC

To reflect the progressive damage of the RSC due to traffic loading and/or environment corrosions, a proper progressive deterioration model for the RSC is necessary. Based on Paterson's (1986) study, the IRI values at any time since opened to traffic can be calculated as

$$\mathrm{IRI}_t = 1.04e^{\eta \cdot t} \cdot \mathrm{IRI}_0 + 263(1 + \mathrm{SNC})^{-5}(\mathrm{CESAL})_t \tag{9}$$

where IRI_t is the IRI value at time t; IRI_0 is the initial roughness value before opened to traffic; t is the time in years; η is the environmental coefficient varying from 0.01 to 0.7 depending on dry or wet and freezing or nonfreezing conditions; the structural number (SNC) is a parameter calculated from the strength and thickness of each layer in the pavement; and $(\mathrm{CESAL})_t$ is the estimated number of traffic in millions in terms of the AASHTO 80-kN (18-kip) equivalent single-axle load at time t. It should be noted that Eq. (9) was initially developed for pavement management systems when initiating the maintenance and rehabilitation of asphalt-surfaced pavements. However, the deterioration of RSCs is affected mainly by three factors: initial roughness level, traffic loading, and age. Other factors, such as pavement thickness and stiffness, have a smaller influence on the roughness deterioration (Shiyab 2007). Therefore, the stiffness difference between bridge pavements and pavements on subgrade was not considered when analyzing the roughness deterioration in this study. Therefore, the RRC at any

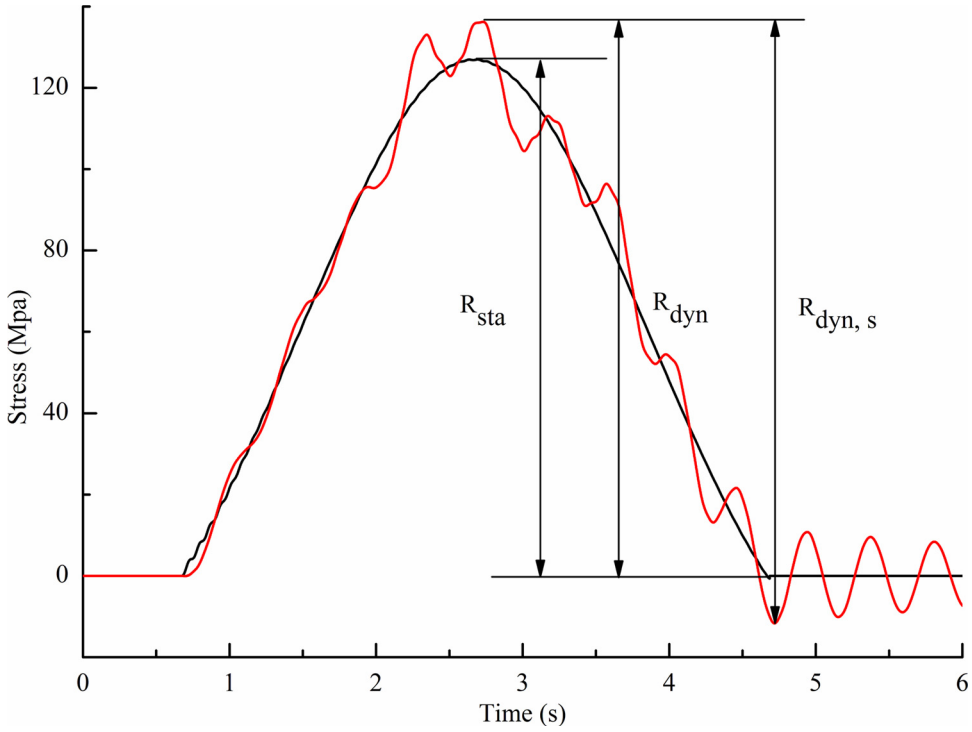

Fig. 4. Definitions of IMs

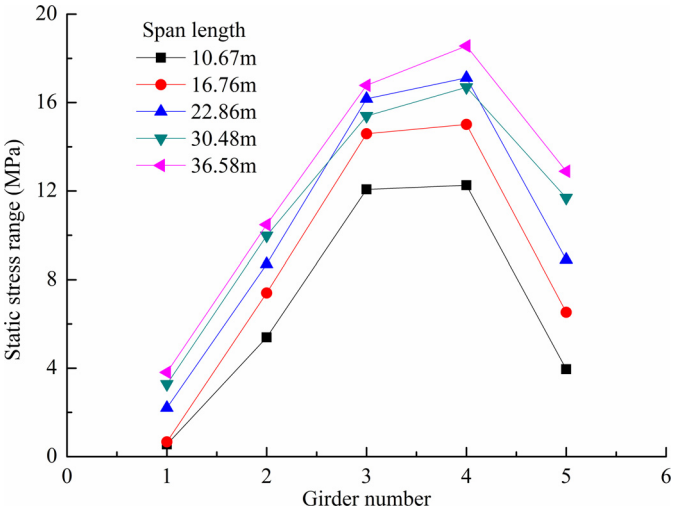

Fig. 5. Maximum static stress ranges at the midspans of the bridges under loading case considered

time since opened to traffic can be predicted with the following equation:

$$\varphi(n_0)_t = 6.1972 \times 10^{-9} \times \exp\{[1.04e^{\eta t} \cdot \mathrm{IRI}_0 + 263(1+\mathrm{SNC})^{-5}(\mathrm{CESAL})_t]/0.42808\} + 2 \times 10^{-6} \quad (10)$$

The purpose of modeling the deterioration process of the RSC is to obtain the required number of truck passages, N_i ($i = 1, 2, 3, 4, 5$), taken for the RSC to deteriorate from one class to another. For instance, N_1 is the number of truck passages required for the RSC to deteriorate from the very good class to the good class. Based on Shiyab (2007), the SNC is calculated to be 6.19, and η is usually adopted as 0.1 for bridges exposed in general environment. In this study, the average daily truck traffic (ADTT) and fraction of traffic in a single lane were assumed to be 2,000 and 0.85, respectively, as suggested by the AASHTO LRFD code (AASHTO 2012). The traffic increase rate was not considered, and thus the CESAL was assumed to be 12.42 for each lane each year (Shiyab 2007). Based on Eq. (10), the deterioration process of the RSC can be analyzed, and the results are shown in Table 4. In Table 4, N_i and t_i are the number of truck passages required and years taken for each class of RSC to deteriorate to the next class, respectively; T is the total years taken for the RSC to deteriorate to the end of each class of the RSC since opened to traffic; and $r_i = N_i/\sum N_i$, ($i = 1, 2, 3, 4, 5$), the proportion of the number of truck passages required for each class of RSC to deteriorate to the next class.

Numerical Studies

In the literature, the influence of a number of parameters on the dynamic IM has been studied, including the vehicle loading position, vehicle weight, vehicle traveling speed, number of loading lanes, RSC, and road-surface roughness correlation (Chang and Lee 1994; Liu et al. 2002; Yang et al. 1995). In this study, three important parameters commonly considered to have a significant effect on the IM were investigated: bridge span length, vehicle speed, and RSC.

It should be noted that the accuracy and reliability of the vehicle–bridge model used in this study were verified in other works (Deng 2009; Deng and Cai 2010c), in which a series of field tests were conducted on an existing slab-on-girder concrete bridge in Louisiana. It was found that the field-measured bridge responses agreed very well with the numerical simulation results.

The span lengths and other parameters of the five bridges used in this study are listed in Table 1. Seven vehicle speeds, ranging from 30 to 120 km/h with an interval of 15 km/h, were considered, and

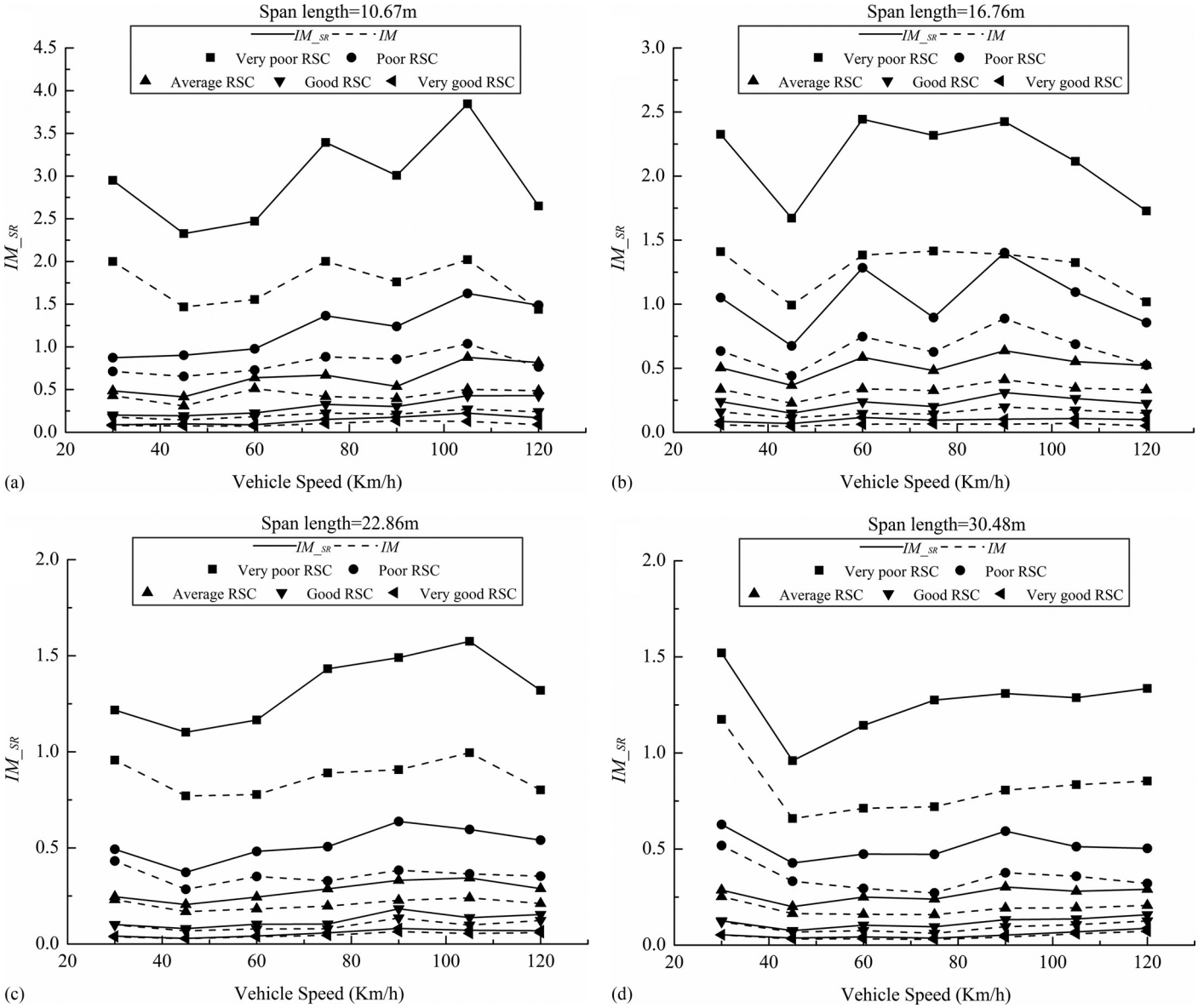

Fig. 6. Variation of IMs with change in vehicle speed and RSC for different bridges under loading case considered

five different RSCs according to ISO (1995) were studied: very good, good, average, poor, and very poor. Fig. 1 shows the vehicle position for the loading case specified in the AASHTO LRFD code (AASHTO 2012), where the vehicle travels along the centerline of the lane. It should be noted that the road surface profiles along left-wheel and right-wheel tracks of the truck were assumed to be exactly the same. In other words, the variation of road surface in the lateral direction was not considered in this study. Actually, it was shown by Liu et al. (2002) that, in practice, the use of two identical profiles does not cause much deviation in the resulting dynamic bridge responses. It should also be noted that the IM due to the fatigue truck may not necessarily equal the IM due to the real traffic (the former is usually slightly larger than the latter). Actually, the fatigue truck adopted in the current AASHTO LRFD code (AASHTO 2012) was developed based on the actual truck-traffic spectrum obtained from weigh-in-motion studies, in which data of more than 27,000 trucks and 30 sites around the United States (Snyder et al. 1985) were collected. A fatigue truck is typically used to represent the equivalent fatigue damage accumulation resulting from the truck traffic at a specific site with a variety of gross vehicle weights and axle configurations (Chotickai and Bowman 2006). Because of this reason, the IM due to the fatigue truck is usually used to represent the IM for the real traffic by researchers for the sake of simplicity and conservativeness.

To investigate the relationship among the three parameters and the IM, for each specific case with a given bridge span length, vehicle speed, and RSC, the vehicle–bridge interaction analysis was set to run 20 times with 20 sets of randomly generated road surface profiles under the given RSC. Then, the average value of the 20 IMs was obtained and used in the following result analysis. A total of 20 simulations were also considered to be sufficient by other researchers (Liu et al. 2002).

Stress range is a key parameter that affects the fatigue behavior of steel bridges. As illustrated in Fig. 4, the $IM_{\_SR}$ is defined as follows (Patrick et al. 1992):

$$IM_{\_SR} = \frac{R_{dyn,s} - R_{sta}}{R_{sta}} \tag{11}$$

whereas the traditional IM is defined using stress as follows:

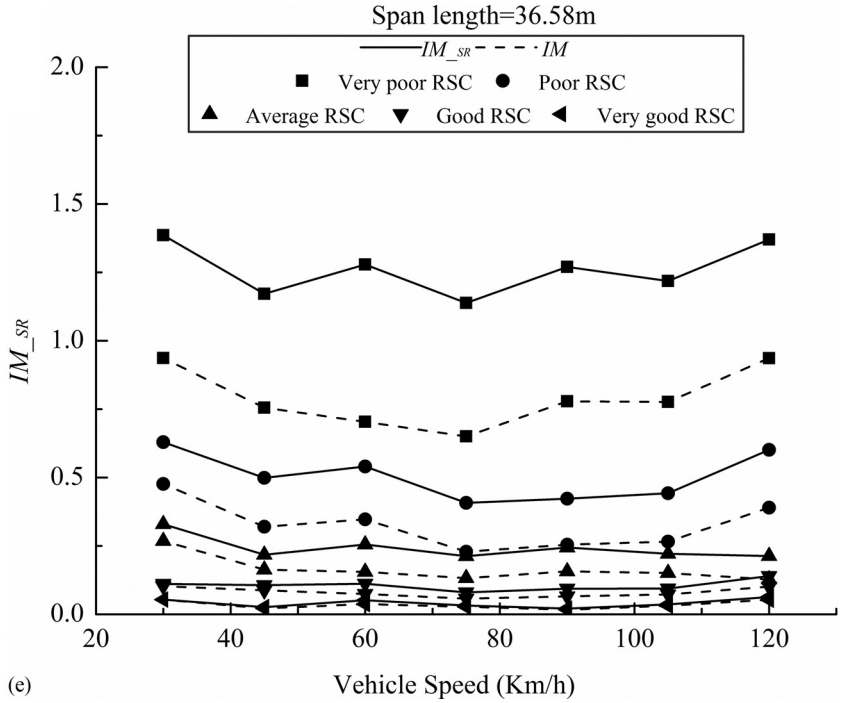

Fig. 6. (*Continued.*)

$$\mathrm{IM} = \frac{R_{\mathrm{dyn}} - R_{\mathrm{sta}}}{R_{\mathrm{sta}}} \tag{12}$$

where $R_{\mathrm{dyn,s}}$, R_{dyn}, and R_{sta} are the maximum dynamic stress range and maximum dynamic stress and static stress caused by the vehicle loading, respectively. The stress range at the midspan of the girder carrying the largest amount of load was selected as the bridge response for calculating the IMs in this study. It should be noted that the numerical simulation results show that the maximum dynamic stress either occurred at the midspan or was very close to the dynamic stress at the midspan, depending on factors including the bridge span length, diaphragm position, vehicle speed, and RSC. Therefore, for the purpose of convenience, the stress at the midspan was chosen in the analysis.

Fig. 5 shows the maximum static stress ranges at the midspan of all five girders of each bridge under the loading case considered. It can be easily seen that the largest stress range occurred at the midspan of Girder 4. Therefore, the stress ranges of Girder 4 were used for calculating the $\mathrm{IM\__{SR}}$. It should be noted that the reason why the stress ranges of Bridge 3 were larger than those of Bridge 4 on Girders 3 and 4 is that Bridge 4 has a diaphragm right at the midspan; thus, the vehicle loading is distributed more evenly laterally.

The average $\mathrm{IMs\__{SR}}$ obtained from the numerical simulations for each RSC based on Eq. (11) were plotted against the vehicle speed in Fig. 6, where the results for bridges with different span lengths were plotted separately. For comparison, the average IMs calculated based on Eq. (12) were also plotted in Fig. 6.

With the average $\mathrm{IMs\__{SR}}$ varying from greater than 3.0 when the RSC is very poor to less than 0.10 when the RSC is very good, it is evident from Fig. 6 that, for all five bridges, the RSC has a significant impact on both the $\mathrm{IMs\__{SR}}$ and the traditional IMs. However, an increase in vehicle speed does not necessarily lead to an increase in the IM, as also reported by other researchers (Brady et al. 2006; Liu et al. 2002). Interestingly, Fig. 6 also shows that the RSC has a greater impact on the $\mathrm{IMs\__{SR}}$ than on the traditional IMs, and the average $\mathrm{IMs\__{SR}}$ are larger than the average traditional IMs under each RSC.

To examine the effect of each parameter on the $\mathrm{IM\__{SR}}$ more clearly, the average $\mathrm{IM\__{SR}}$ were plotted against each of the three parameters separately in Fig. 7. It can be easily seen that the average $\mathrm{IMs\__{SR}}$ for all the RSCs are all above the AASHTO-specified value of 0.15 with the exception of the very good RSC. This is easily understandable because the value of 0.15 adopted in the AASHTO LRFD code for fatigue design is based on the study of Hwang and Nowak (1991), in which only an average RSC was considered in the numerical simulations.

To propose rational $\mathrm{IMs\__{FD}}$ for steel I-girder bridges, the following steps were taken. First, based on the regression analysis on the simulation results, the expressions for predicting the $\mathrm{IM\__{SR}}$ for each RSC were obtained. Then, by considering the cumulative fatigue damage caused by the passage of each truck under different RSCs and the number of truck passages taken to cause the RSC to deteriorate from one class to the next, the $\mathrm{IMs\__{FD}}$ for steel I-girder bridges were proposed, taking into consideration the whole lifecycle of the RSC.

Because it has been demonstrated that the $\mathrm{IM\__{SR}}$ is highly dependent on the RSC, it would be natural to express the $\mathrm{IM\__{SR}}$ as a function of RSC. In this study, the following expressions for predicting the $\mathrm{IM\__{SR}}$ under each RSC were suggested based on a regression analysis:

$$\mathrm{IM\__{SR}}_i = \mathrm{RSI}_i \times \begin{cases} 0.46 + 0.057 \times (22.86 - L) & L < 22.86\,\mathrm{m} \\ 0.46 & L \geq 22.86\,\mathrm{m} \end{cases} \tag{13}$$

where RSI_i = road surface index, which is taken as 0.12, 0.27, 0.62, 1.21, or 2.71, corresponding to very good, good, average, poor, or very poor RSC, respectively, based on the regression analysis results; and L = bridge span length.

The reason why vehicle speed was not considered in this expression is that vehicles can usually run at speeds within a wide range,

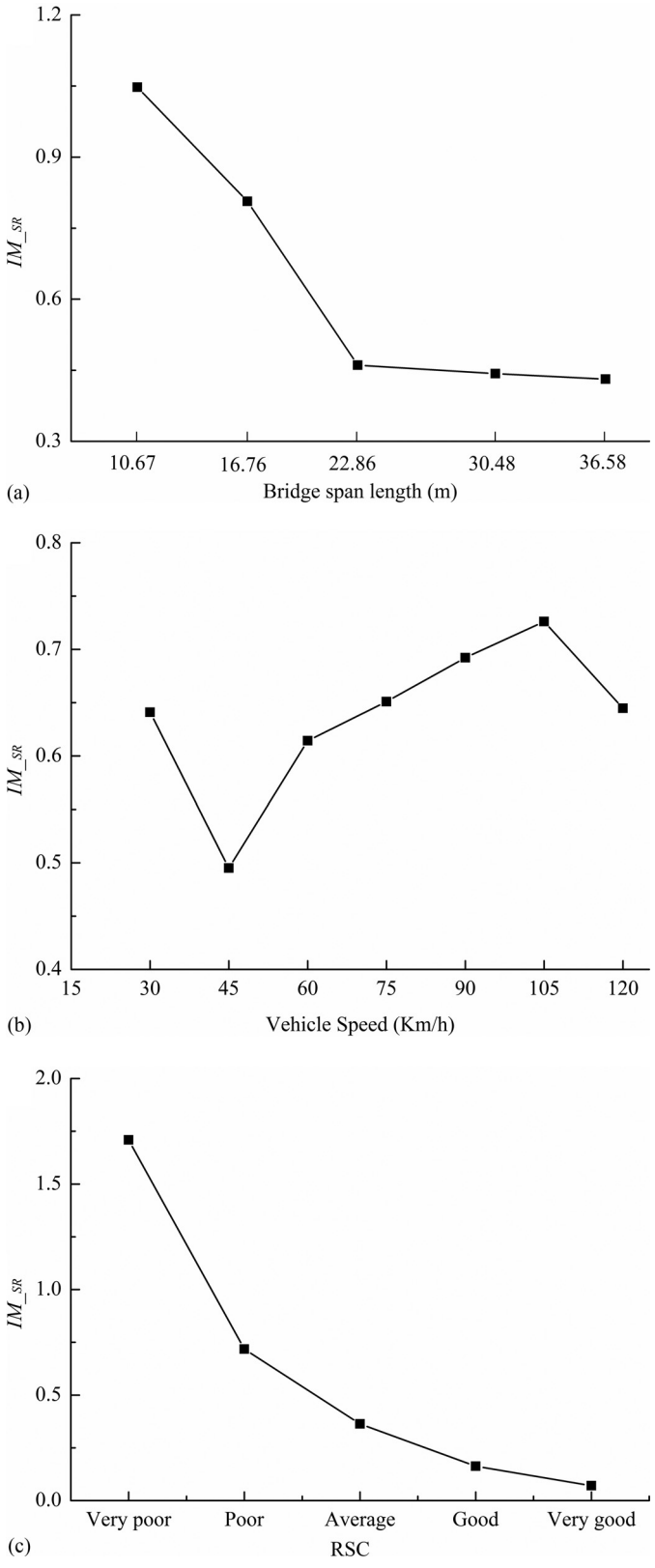

Fig. 7. Variation of the average $IM_{\_SR}$ with change of each parameter: (a) bridge span length; (b) vehicle speed; (c) RSC

whereas an increase in vehicle speed does not necessarily cause the $IM_{\_SR}$ to increase or decrease monotonically, as shown in Fig. 6. Moreover, the influence of vehicle speed on the $IM_{\_SR}$ is considerably smaller than that of bridge span length and RSC. Therefore, as usually done in the codes, vehicle velocity is not included as a variable in the proposed expressions for predicting the $IM_{\_SR}$. In addition, it should also be noted that, in real life, drivers tend to drive at lower speeds under worse RSCs, and therefore it may not be appropriate to calculate the average IMs for each RSC by taking the average of the results for all seven vehicle speeds considered. However, due to the same reasons discussed above, this influence was not considered in this study.

Table 5. $IMs_{\_SR}$ for the Six Bridges

	RSC				
Bridge	Very poor	Poor	Average	Good	Very good
1	3.13	1.40	0.72	0.31	0.14
2	2.18	0.98	0.50	0.22	0.10
3–5	1.25	0.56	0.29	0.13	0.06
6	2.17	0.96	0.52	0.21	0.10

Based on the proposed expressions, the $IMs_{\_SR}$ of the five bridges studied were predicted for each RSC, as summarized in Table 5.

To evaluate the credibility of the proposed $IM_{\_SR}$ for each RSC, another bridge model (Bridge 6) with a different bridge width from the previous five bridges was built. This bridge has the same span length as Bridge 2 (16.76 m), whereas its configuration was slightly modified from Bridge 2 by adding two more girders to Bridge 2, leading to an increased bridge width of 14.92 m (49 ft). The $IM_{\_SR}$ of Bridge 6 was then investigated using the five different RSCs and seven speeds. Again, for each RSC and vehicle speed, the program was set to run 20 times with randomly generated road surface profiles, resulting in 140 $IM_{\_SR}$ values under each RSC for the bridge. Table 5 summarizes the average $IMs_{\_SR}$ of the bridge for each RSC. The results show that the predicted $IMs_{\_SR}$ of Bridge 6 are very close to those of Bridge 2 predicted using the proposed expression, confirming that the proposed expressions for predicting $IMs_{\_SR}$ may be used for steel I-girder bridges with different bridge widths.

Proposed $IMs_{\_FD}$

As fatigue failure is related to the cumulative damage caused by the passage of each truck, a reasonable $IM_{\_FD}$ should take into consideration the effect of each truck passage on the cumulative fatigue damage during the lifecycle of the bridge. Based on this consideration, the following IMs were proposed for the fatigue design of steel I-girder bridges under the traffic and environmental conditions suggested by the AASHTO LRFD code:

$$\mathrm{IM}_{\mathrm{FD}} = \sum r_i \times \mathrm{IM}_{\mathrm{SR}i} = \sum r_i \times \mathrm{RSI}_i \times \begin{cases} 0.46 + 0.057 \times (22.86 - L) & L < 22.86\,\mathrm{m} \\ 0.46 & L \geq 22.86\,\mathrm{m} \end{cases} \quad (14)$$

where r_i (i = 1, 2, 3, 4, 5) is the ratio of the numbers of truck passages needed for each class of the RSC to deteriorate to the next class, as summarized in Table 4.

Based on Eq. (14), the proposed $IMs_{\_FD}$ for the five bridges studied were calculated and are summarized in Table 6. It should be noted that, in Table 6, that two conditions were considered: Condition A and Condition B, where the only difference between the two conditions is that Condition A included all five RSCs when calculating the $IM_{\_FD}$ using Eq. (14), whereas Condition B does not include the *very poor* RSC in the calculation. The purpose of not

Table 6. $IMs_{\_FD}$ for the Five Bridges

Bridge	Span length (m)	$IM_{\_FD}$	
		Condition A	Condition B
1	10.67	0.66	0.36
2	16.76	0.46	0.25
3	22.86	0.26	0.14
4	30.48	0.26	0.14
5	36.58	0.26	0.14

Note: In Condition A, all five RSCs were considered, i.e., very poor, poor, average, good, and very good. In Condition B, all five RSCs were considered except the very poor RSC.

considering the very poor RSC in Condition B is that, in real life, maintenance has usually been performed before the road-wearing surface turns into a very poor condition. Therefore, Condition B may be more realistic when considering the whole lifecycle of the road-wearing surface.

Table 6 shows that the proposed $IMs_{\_FD}$ for relatively short bridges (Bridges 1 and 2) are significantly larger than those for relatively long bridges (Bridges 3–5). In addition, the $IMs_{\_FD}$ under Condition A are considerably larger than those under Condition B, indicating the importance of maintaining the RSC, especially *very poor* RSC, in reducing the fatigue damage of bridge components due to the traffic load. It is also very interesting to note that, for bridges with span lengths of no shorter than 22.86 m (Bridges 3–5), the proposed $IM_{\_FD}$ under Condition B has a constant value of 0.14, which is slightly smaller than the IM of 0.15 specified in the AASHTO LRFD code (AASHTO 2012) for fatigue design. This indicates that the IM of 0.15 specified in the current AASHTO LRFD code is suitable for the fatigue design of medium-span to long-span simply supported steel I-girder bridges. However, for the fatigue design of short-span bridges, larger IMs should be adopted.

Conclusions

In this study, the $IMs_{\_SR}$ for steel I-girder bridges were studied. Simple and reasonable $IMs_{\_FD}$ for steel I-girder bridges were proposed by considering the cumulative fatigue damage caused by the passage of each truck under different RSCs and the deterioration process of the road surface during its whole lifecycle. Whereas previous researchers who have based their studies on either numerical simulation or field test results have raised the concern that the IM currently adopted for fatigue design may be unconservative under certain circumstances, this paper attempted to provide more reliable quantitative results that can more accurately describe the relationships between the IM and its influencing parameters and simple IMs that can be used as reference by researchers and engineers. Based on the results from this study, the following conclusions can be drawn:

1. Under the traffic and environment conditions suggested by the AASHTO LRFD code, it takes 12.6 years for the RSC to deteriorate from the very good class to the very poor class. The time taken for the RSC to deteriorate from one class to the next class becomes shorter as the RSC becomes worse.
2. The RSC has a greater impact on the $IMs_{\_SR}$ than on the traditional IMs calculated using the maximum stress, and the average $IMs_{\_SR}$ are larger than the average traditional IMs under each RSC.
3. The proposed $IMs_{\_FD}$ for steel I-girder bridges can more accurately consider the dynamic effect of vehicle loading on the fatigue life of steel I-girder bridges. The proposed IMs also indicate that the IM of 0.15 adopted in the current AASHTO LRFD code is still suitable for the fatigue design of medium-span to long-span steel I-girder bridges under the assumed traffic and environmental condition. However, for the fatigue design of short-span steel bridges, larger IMs should be adopted.

It should be noted that the expression for $IM_{\_FD}$ in Eq. (14) was obtained with an ADTT of 2,000 under the environmental condition suggested by the AASHTO LRFD code. Therefore, IMs calculated using Eq. (14) can be used as supplementary specifications to the AASHTO LRFD bridge design specifications when dealing with fatigue design of short steel bridges under the assumed traffic and environmental conditions. However, the method proposed in this study can be used for determining reasonable $IMs_{\_FD}$ for different types of steel bridges and under different traffic and environmental conditions by adopting different environmental coefficients (η) and traffic numbers (CESAL) in Eq. (10).

Acknowledgments

The authors acknowledge financial support provided by the National Natural Science Foundation of China (Grants 51208189 and 51478176) and the Excellent Youth Foundation of Hunan Scientific Committee (Grant 14JJ1014).

References

AASHTO. (2012). *LRFD bridge construction specifications*, 3rd Ed., Washington, DC.

ANSYS 14.5 [Computer software]. ANSYS, Canonsburg, PA.

Brady, S. P., O'Brien, E. J., and Žnidarič, A. (2006). "Effect of vehicle velocity on the dynamic amplification of a vehicle crossing a simply supported bridge." *J. Bridge Eng.*, 10.1061/(ASCE)1084-0702(2006)11:2(241), 241–249.

Chang, D., and Lee, H. (1994). "Impact factors for simple-span highway girder bridges." *J. Struct. Eng.*, 10.1061/(ASCE)0733-9445(1994)120:3(704), 704–715.

Chotickai, P., and Bowman, M. D. (2006). "Truck models for improved fatigue life predictions of steel bridges." *J. Bridge Eng.*, 10.1061/(ASCE)1084-0702(2006)11:1(71), 71–80.

da Silva, J. D. S. (2004). "Dynamical performance of highway bridge decks with irregular pavement surface." *Comput. Struct.*, 82(11–12), 871–881.

Deng, L. (2009). "System identification of bridge and vehicle based on their coupled vibration." Ph.D. thesis, Louisiana State Univ., Baton Rouge, LA.

Deng, L., and Cai, C. S. (2009). "Identification of parameters of vehicles moving on bridges." *Eng. Struct.*, 31(10), 2474–2485.

Deng, L., and Cai, C. S. (2010a). "Development of dynamic impact factor for performance evaluation of existing multi-girder concrete bridges." *Eng. Struct.*, 32(1), 21–31.

Deng, L., and Cai, C. S. (2010b). "Identification of dynamic vehicular axle loads: theory and simulations." *J. Vib. Control*, 16(14), 2167–2194.

Deng, L., and Cai, C. S. (2010c). "Bridge model updating using response surface method and genetic algorithm." *J. Bridge Eng.*, 10.1061/(ASCE)BE.1943-5592.0000092, 553–564.

Dodds, C., and Robson, J. (1973). "The description of road surface roughness." *J. Sound Vib.*, 31(2), 175–183.

Huang, D., and Wang, T.-L. (1992). "Impact analysis of cable-stayed bridges." *Comput. Struct.*, 43(5), 897–908.

Hwang, E.-S., and Nowak, A. S. (1991). "Simulation of dynamic load for bridges." *J. Struct. Eng.*, 10.1061/(ASCE)0733-9445(1991)117:5(1413), 1413–1434.

ISO. (1995). "Mechanical vibration—Road surface profiles—Reporting of measured data." *ISO 8068:(E)*, Geneva.

Jaksic, V., Connor, A. O., and Pakrashi, V. (2014). "Damage detection and calibration from beam–moving oscillator interaction employing surface roughness." *J. Sound Vib.*, 333(17), 3917–3930.
Liu, C., Huang, D., and Wang, T.-L. (2002). "Analytical dynamic impact study based on correlated road roughness." *Comput. Struct.*, 80(20), 1639–1650.
O'Brien, E., Li, Y., and González, A. (2006). "Bridge roughness index as an indicator of bridge dynamic amplification." *Comput. Struct.*, 84(12), 759–769.
Paterson, W. D. (1986). "International roughness index: Relationship to other measures of roughness and riding quality." *Transportation Research Record*, 1084, 49–59.
Patrick, P., Omar, C., and Jean, P. (1992). "Bridge dynamics and dynamic amplification factors—A review of analytical and experimental findings." *Can. J. Civ. Eng.*, 19(2), 260–278.
Rao, V., and Talukdar, S. (2003). "Prediction of fatigue life of a continuous bridge girder based on vehicle induced stress history." *Shock Vib.*, 10(5), 325–338.
Sayers, M., and Karamihas, S. (2007). *The little book of profiling: Basic information about measuring and interpreting road profiles*, Univ. of Michigan, Ann Arbor, MI.
Schenk, C. A., and Bergman, L. A. (2003). "Response of continuous system with stochastically varying surface roughness to moving load." *J. Eng. Mech.*, 10.1061/(ASCE)0733-9399(2003)129:7(759), 759–768.
Shi, X. (2006). "Structural performance of approach slab and its effect on vehicle induced bridge dynamic response." Ph.D. thesis, Louisiana State Univ., Baton Rouge, LA.
Shiyab, A. (2007). "Optimum use of the flexible pavement condition indicators in pavement management system." Ph.D. thesis, Curtin Univ. of Technology, Perth, Australia.
Snyder, R. E., Likins, G. E., and Moses, F. (1985). "Loading spectrum experienced by bridge structures in the United States." *Rep. No. FHWA/RD-85/012*, Bridge Weighing Systems Inc., Warrensville, OH.
Wu, S. Q., and Law, S. S. (2011). "Vehicle axle load identification on bridge deck with irregular road surface profile." *Eng. Struct.*, 33(2), 591–601.
Yang, Y.-B., Liao, S.-S., and Lin, B.-H. (1995). "Impact formulas for vehicles moving over simple and continuous beams." *J. Struct. Eng.*, 10.1061/(ASCE)0733-9445(1995)121:11(1644), 1644–1650.
Zhang, W., and Cai, C. S. (2012). "Fatigue reliability assessment for existing bridges considering vehicle speed and road surface conditions." *J. Bridge Eng.*, 10.1061/(ASCE)BE.1943-5592.0000272, 443–453.
Zhang, W., and Cai, C. S. (2013). "Reliability-based dynamic amplification factor on stress ranges for fatigue design of existing bridges." *J. Bridge Eng.*, 10.1061/(ASCE)BE.1943-5592.0000387, 538–552.